Biomass and Bioenergy 107 (2017) 135–149

Contents lists available at ScienceDirect

Biomass and Bioenergy

journal homepage: http://www.elsevier.com/locate/biombioe

Research paper

Fluid dynamic study of mixtures of sugarcane bagasse and sand particles: Minimum fluidization velocity

Nestor Proenza Pérez [a, *], Daniel Travieso Pedroso [b, c], Einara Blanco Machin [c], Julio Santana Antunes [c], Ricardo Alan Verdú Ramos [d], Jose Luz Silveira [c]

[a] Federal Center of Technological Education Celso Suckow da Fonseca (CEFET/RJ), Angra dos Reis Campus, Brazil
[b] Technological Development Unit-UDT, University of Concepcion, Coronel, Chile
[c] São Paulo State University, Faculty of Engineering at Guaratinguetá, Department of Energy, Laboratory of Optimization Energetic Systems (LOSE), Brazil
[d] São Paulo State University, Faculty of Engineering at Ilha Solteira, Institute of Bioenergy Research (IPBEN-UNESP), Brazil

ARTICLE INFO

Article history:
Received 11 February 2017
Received in revised form
31 July 2017
Accepted 9 August 2017
Available online 16 October 2017

Keywords:
Biomass sand mixture
Minimum fluidization velocity
Fluidized bed
Segregation

ABSTRACT

This paper is focused on the study of fluid-dynamic behavior of mixtures of the sugarcane bagasse particles and quartz sand in a transparent fluidized bed column. The minimum fluidization velocity (V_{mf}) was determined by different mean particle diameters and different mass fractions in the mixture compositions. The values of V_{mf} increased with amount of biomass in the mixture increased as well as with the size of the biomass particles in the range of $9.5 \geq d_{pb} > 0.225$ mm. Binary mixtures with diameter ratios biomass/sand ≤ 1 had a (V_{mf}) almost constant as a function of mass fraction of biomass. It is suggested a practical upper limit of biomass fraction in the mixtures less than 5% of the overall bed mass to obtain a good mixing and uniform distribution in the bed. New correlations were developed to predict the values of (V_{mf}). It was found that the present proposed correlation predicted the (V_{mf}) for binary mixtures of sugarcane bagasse and sand particles more accurately than other correlations reported in the literature available.

1. Introduction

The use for energy purposes of biomass materials using fluidized bed technology has reached grounds recently due to the advantages of this type of process [1,2]. The use of fluidized bed has been widely used in processes involving gasification, pyrolysis and combustion of a wide range of particular materials including biomass, [3–6].

Many of these processes are based on fluidization, but the particles of biomass, especially those with very irregular shapes, such as sugarcane bagasse, are very difficult to fluidize alone as it is already known, due to their peculiar shapes, variety of sizes and density (e.g. long thin particles, low density and very irregular shape) [7,8], which is generally added to an inert material to facilitate and improve fluidization (e.g. sand, alumina, etc.) [9]. This inert material, at the same time, brings about an increase in the heat transfer coefficient, increasing the rate of heat exchange [10], improving the yield of gasification, pyrolysis and combustion processes.

The fluid-dynamic behavior of binary mixtures of sand and biomass is strongly influenced by the differences of the distributions of shape, size and density of particles [11], often it propitiates a segregation, which is characterized by a downward motion towards the base of the bed particles of higher density, such as sand, while the solid of lower density, usually biomass particles, float on the top of the bed [11], being called the *jetsam* and *flotsam* respectively [12].

Accordingly, the fluid-dynamic characteristics, including the minimum fluidization velocity, mixing, segregation and residence time, are of great interest to the design and optimization of processes in the fluidized bed equipment [7]. The minimum fluidization velocity is definitely the most important parameter in fluidization processes [13], the knowledge of this parameter is of vital importance to a proper design and operation of fluid bed equipment [14–16].

Several studies have been developed to investigate the fluid-dynamic characteristics of mixtures of inert and biomass materials. Rao and Bheemarasetti [17] reported a study evaluating the influence of the weight ratio biomass/inert and the size of inert material, using different types of biomasses. An increase of the

* Corresponding author.
E-mail address: nestor.perez@cefet-rj.br (N.P. Pérez).

https://doi.org/10.1016/j.biombioe.2017.08.015
0961-9534/

Nomenclature

A_{pe}	sphere area (m^2)
A_r	Archimedes number (-)
A_c	cross-sectional area (m^2)
a	width (m)
d_{pm}	effective particle diameter of mixture (m)
$\overline{d}_p$	Sauter mean diameter (m)
d_p	particle diameter (m)
d_{pin}	inert particle diameter (m)
d_{pb}	biomass particle diameter (m)
d_{tp}	Feret's diameter (m)
g	gravity (m/s^2)
H	height (m)
L	length (m)
ΔP	drop pressure (Pa)
R_e	Reynolds number (-)
V_{sg}	superficial air velocity (m/s)
V_{if}	incipient fluidization velocity (m/s)
V_{cf}	complete fluidization velocity (m/s)
V_{mf}	minimum fluidization velocity (m/s)
W	weigh of bed material (kg)
X	mass fraction of particles (%)
X_b	weight percentage of biomass (−)
X_{in}	weight percentage of inert (−)
D_c	column diameter

Subscript

b	biomass
i	each parameter
in	inert
g	gas
t	theoretical
f	fixed bed
m	mixture
fl	*flotsam*
j	*jetsam*
mf	minimum fluidization

Greek symbols

ε	voidage (-)
ρ_p	particle density (kg/m^3)
ρ_r	real or skeletal density (kg/m^3)
ρ_{bulk}	bulk density (kg/m^3)
ρ_b	particle density of biomass (kg/m^3)
ρ_{in}	particle density of inert (kg/m^3)
ρ_{pm}	effective particle density of mixture (kg/m^3)
ϕ	sphericity (-)
μ	viscosity (Pa.s)

fraction by mass of biomass causes an increase in the minimum fluidization velocity, and an increase in the diameter of the sand almost doubles the value of the (V_{mf}) for fractions up to 10% of biomass in the binary mixture. The authors propose a new correlation for determining the (V_{mf}) of mixtures biomass/sand, based on density properties and effective diameter of the mixture, showing good correlation with experimental results.

Similar studies have been reported by Aznar et al. [18] using different biomasses like thinning pine, cereal straw and wood chips of various sizes, sawdust, and ground thistle, mixed with beach and silica sands, dolomite and commercial catalytic cracking catalyst. These authors determined an increase of (V_{mf}) when the volume fraction of biomass in the mixture was increased. They also determined that the existing conventional correlations for binary mixtures do not predict satisfactorily this parameter due to its limitations, especially for binary mixtures biomass/sand.

Cook et al. [19] studied binary mixtures of palm shell particles with different size and of different types and sizes of sand, showing that the (V_{mf}) remains practically constant for different fractions of biomass/sand when the particle diameters are too small (particles of palm shell between 1.18 and 2.36 mm with 2–10% of biomass in the mixture and sand of 0.196 mm of diameter). Rao and Reddy [13] also studied the fluid-dynamic characteristics of mixtures of rice husk, sawdust, and groundnut shells and sand with different sizes, making comparisons between experimental and theoretical values obtained from different correlations. Concluding that the correlation proposed by Todes [20] was the most suitable to predict the (V_{mf}) of the studied biomasses.

Remake et al. [21] analyzed the fluidization behavior for wood/sand mixtures. Experimental results of minimum fluidization velocity were compared with many correlations found in the literature, showing in all cases, that correlations underestimate or overestimate around 50% the experimental value. Further experiments are recommended to get a correlation to predict this parameter correctly. Paudel and Feng [8] developed a new correlation for mixtures of walnut shell and corn cob with sand, glass bead and alumina, based on forty-five sets of experimental data found in the literature. This correlation takes into account the biomass weight percentage, the predicted results showed good agreement with the experimental results.

Woh et al. [22] studied the effects of the size of the palm kernel cake particle, they assumed the (V_{mf}) increases as diameter increases. Si and Guo [23] proposed a new correlation for mixtures of biomass/sand, taking into account the sphericity of the particles. Another study using mixtures of wood chip, mung beans, millet, corn stalk, cotton stalk and with different bed materials (silica sand, continental flood basalt (CFB) cinder, and alumina) was reported by Zhong et al. [7]. They determined that the minimum fluidization velocity of long thin biomass, increases, with an increase of diameter and aspect ratio (length/diameter) of biomass particles, and for binary mixtures, the (V_{mf}) increases as increasing weight percentage of biomass particles, as well as with an increase of diameter and density of inert particles. Two new correlations were proposed which take into account the effective density and diameter of the mixture.

Although many studies of mixtures of biomass and inert material has been developed in recent years, most of them have focused on the influence of the diameter of the inert material and the mass fraction of biomass on (V_{mf}), but very few studies have evaluated the influence of the physical and geometrical properties of biomass particles with extreme forms (e.g. long thin particles with low density) such as sugarcane bagasse.

The results have shown that the predicted values for the (V_{mf}) are far from experimental values, due to the phenomena of segregation, poor quality of fluidization and emergence of preferential channels, so that more experimental studies on fluid-dynamic behavior of binary mixtures of extreme biomasses (e.g. sugarcane bagasse) and inert particles like quartz sand are still needed, in order to understand the influence of important properties of the particles as size distribution, extreme forms and low densities.

In this context the aim of this study is to evaluate the influence of the size and mass fraction of sugarcane bagasse particles mixed with quartz sand, the minimum fluidization velocity as well as the segregation of the mixture in order to find suitable ranges of fluidization that allow the design and proper functioning of fluidized bed technologies. It is also intended to make a comparison of experimental data of minimum fluidization velocity with different correlations already stated in literature and develop a new correlation that fit better to the specific characteristics of this type of biomass.

2. Materials and methods

2.1. Preparation of materials

A sample of approximately 150 kg of sugarcane bagasse (belonging to the genus *Saccharum*) was collected in the Serra mill, located in the central region of São Paulo (−22.012436, −48.000392). The bagasse comes from the harvesting season 2014-2015 with sugarcane age between 12 and 14 months. The sample consist of mixtures of different varieties of sugarcane like SP 91-1049, RB 867515, RB 965902, RB 966928 and SP83-2847, which are the varieties most used in Brazil and mainly in the region of Sao Paulo and the Brazilian northeastern [24]. In the mill, the sugarcane bagasse is storage in form of stack. The sample was collected from the ends and center of the stack and placed in plastic bags of 100 L of capacity. The collected samples were mixed and divided, a quarter of this mixture was storage in a plastic bags and hermetically sealed for use in the experiments. The rest of the bagasse was carefully stored at room conditions in sealed plastic bags. Was considered bagasse sample "*in natura*" the sample with the composition and physical characteristics that the bagasse have, without any pretreatment processes like sieving and with the equilibrium moisture, to differentiate it, from the other bagasse particles obtained from the granulometric analysis.

The inert material used, in this case, was quartz sand with a basic composition of silicon dioxide of white color and physico-chemical characteristics detailed in Table 1.

2.2. Properties of the materials

The determination of the granulometric composition of each of the particles used in this study (sand and sugarcane bagasse) was performed in a sieve machine Produtest, model T, using a Tyler standard mesh series for the characterization of particle with sizes of 9.5, 4.75, 2.36, 1.18, 0.59, 0.3, 0.15 milimeters respectively. The average diameter of each sample composed of different particle sizes was determined as Kunii and Levespiel [25], and Geldart [26]:

$$\overline{d}_p = \left[\frac{1}{\sum_{i=1}^{n}\left(\frac{x_i}{d_{p,i}}\right)}\right] \tag{1}$$

where x_i is the mass fraction of particles with an average diameter equal to *dpi* and *dpi* is the mean value between the aperture of the sieve that allowed that fraction to pass through, and that of the sieve that retained the fraction, defined as [27]:

$$d_{pi} = \left[\frac{\left(X_i^2 + X_{i+1}^2\right)\cdot(X_i + X_{i+1})}{4}\right]^{0.33} \tag{2}$$

The particle size distribution of sand and sugarcane bagasse are shown in Fig. 1. The mean diameter determined in the sieve analysis for both groups of particles was 0.225 mm and 0.722 mm respectively.

The determination of the real density of the particles was made using a helium gas pycnometer model ULTRAPYC Quantachrome brand 1200e. The bulk density was determined by liquid pycnometry technique. The experiment was performed in triplicate, using water as fluid. The determination of bulk density was performed following the ASTM *Standard Test Method for Bulk Density of Densified Particulate Biomass Fuels* E873-82 [28], and an electronic balance (CELTAC Mark), accuracy of 0.01 g. The porosity of the packed bed is directly related to the bulk density and particle density, for its determination is used the following equation:

$$\varepsilon_{mf} = 1 - \frac{\rho_{bulk}}{\rho_p} \tag{3}$$

The principal geometric parameters of fine sugarcane bagasse particles were made using digital image analysis techniques, in this case, a Zeiss microscope, model Stemi 2000 and the ImageJ, that allow to fit to an ellipse, the binary image projected by the particles; on based on second order central moments [29]. The measurement of principal dimensions of coarse particle was determined according to the Heywood's and Bernhardt description [30,27]. Fiber like particles are measured using an electronic digital caliper and an electronic digital thickness gage both with a resolution of 0.01 mm. The sphericity (ϕ) and the aspect ratio (AR) were determined by equations (3) and (4), following the methodologies reported by Refs. [10,31]:

$$\phi = 4\cdot\frac{A_{pe}}{\pi\cdot(d_{tp})^2} \tag{4}$$

$$AR = \frac{l}{a} \tag{5}$$

Table 2 shows the principal characteristics of sand and biomass particles. Most of the biomass (sugarcane bagasse) particles are larger than inert particles, but less heavy.

2.3. Theoretical analysis

The determination of minimum fluidization velocity in a fluidized bed containing only one component, that is, a bed with a relatively narrow distribution of particle sizes and similar densities is well defined. The pressure drop of a fixed bed with length (L), for non-spherical particles with an average diameter (d_p) is given by Ergun [33] as:

$$\frac{\Delta P}{H_f} = \frac{150\left(1-\varepsilon_f\right)^2}{{\varepsilon_f}^3}\cdot\frac{\mu_g\cdot V_{sg}}{\left(\phi\cdot d_p\right)^2} + \frac{1,75\left(1-\varepsilon_f\right)}{{\varepsilon_f}^3}\cdot\frac{\left(\rho_g\cdot V_f\right)^2}{\left(\phi\cdot d_p\right)} \tag{6}$$

Re-arranging Ergun equation for the point of minimum fluidization a correlation expressed in terms of the dimensionless quantity known as Archimedes number (Ar) and Reynolds number of minimum fluidization (Re_{mf}) is obtained:

Table 1
Main physical - chemical properties of sand.

Chemical analysis		Physical analysis	
Element	% in weight	Characteristic	Variation limit
S_iO_2	98.7	Loss on fire (850 °C)	0.5%
Al_2O_3	0.16	Bulk density (g/cm^3)	1.4–1.6
Fe_2O_3	0.03	PH (aqueous solution 5%)	5.0–10.0
CaO	0.10	Real density (g/cm^3)	2.65–2.9
		Moisture (%)	Maximum 1%

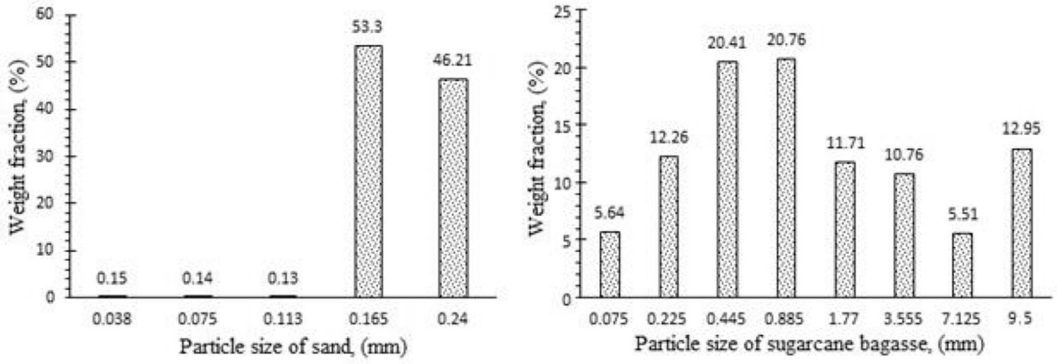

Fig. 1. Size distribution of the particles.

Table 2
Characteristic parameters of particles.

diameter (mm)	ρ_{bulk} (kg/m^3)	ρ_p (kg/m^3)	ρ_r (kg/m^3)	Voidage (ε_{mf})	(ϕ)	*AR*	L/d_{pb}	Geldart [32] Classification
Sand								
0.225	1500	2585.3	2750	0.42	0.78	–	–	B
Bagasse								
9.500	66.25	465.92	1389.48	0.857	0.27	5.508	7.40	D
7.125	74.61	470.56	1401.86	0.841	0.28	5.375	7.12	D
3.555	77.95	478.60	1420.84	0.837	0.32	4.660	6.85	B
1.770	79.30	483.29	1476.08	0.835	0.28	5.429	7.29	B
0.885	82.98	502.67	1542.22	0.834	0.30	5.282	7.86	A
0.722[a]	91.46	484.63	1504.00	0.832	0.39	3.922	–	B
0.445	93.13	520.04	1802.86	0.820	0.34	4.547	6.04	A
0.225	107.04	560.58	1951.70	0.809	0.54	2.227	4.98	A
0.075	147.80	605.21	2221.14	0.755	0.55	2.140	3.47	A

[a] Sugarcane bagasse in natura (composed for all sieve fractions and with mean diameter $\overline{d}_p$).

$$A_r = \frac{150\left(1-\varepsilon_{mf}\right)}{\phi^2 {\varepsilon_{mf}}^3}\cdot R_{emf} + \frac{1,75}{\phi\ {\varepsilon_{mf}}^3}\cdot {R_{emf}}^2 \tag{7}$$

where:

$$A_r = \frac{{d_p}^3\cdot\rho_g\cdot\left(\rho_p-\rho_g\right)\cdot g}{{\mu_g}^2} \tag{8}$$

$$R_{emf} = \frac{d_p\cdot V_{mf}\cdot\rho_g}{\mu_g} \tag{9}$$

In this equation the sphericity of the particle and the porosity of minimum fluidization should be determined, parameters which are very difficult to obtain experimentally. Wen and Yu [31] proposed a simplified form which does not consider these parameters in the form:

$$A_r = 1650\cdot R_{emf} + 24.5\cdot {R_{emf}}^2 \tag{10}$$

or

$$R_{emf} = \left[33.7^2 + 0.0408A_r\right]^{0.5} - 33.7 \tag{11}$$

Both equations, (6) and (10) are designed for a single component, whereby Goossens et al. [35] proposed the following equations to calculate the size and density of particles of a binary mixture.

$$\frac{1}{\rho_{pm}} = \frac{X_b}{\rho_b} + \frac{X_{in}}{\rho_{in}} \tag{12}$$

$$d_{pm} = d_{pin}\cdot d_{pb}\cdot\left(\frac{X_{in}\cdot\rho_b + X_b\cdot\rho_{in}}{X_{in}\cdot\rho_b\cdot d_{pb} + X_b\cdot\rho_{in}\cdot d_{pin}}\right) \tag{13}$$

The determination of the effective density (ρ_{pm}) and the characteristic diameter of the binary mixture (d_{pm}) allowed to determine the minimum fluidization velocity using Reynolds-Archimedes correlations developed for a single component, as it is reported by many researchers [33,37–43].

Other correlations developed specifically for binary systems using biomass are shown in Table 3.

2.4. Experimental installation

The experimental installation is shown in Fig. 2 was made of acrylic Plexiglas with a circular section with an inner diameter of 190 mm (1) and a total height of 3 m. A radial blower (3) supplied air for fluidization of the bed. In the blower outlet there is a control valve (8) with an angular graduate aperture for regulating the air flow. The air distributor (2) was composed of 33 equally spaced nozzle-type tuyeres, each tuyere have four horizontal holes of 2 mm inclined to 45°. The distributor open area was 3.6%. The superficial air velocity was measured with a digital thermo anemometer with a hot-wire sensor, model TAFR-200 (6) with a range of 0–25 m/s and resolution of 0.01 m/s. Four pressure taps (4) for measuring the pressure drop were installed on the wall of the column. To prevent blockage by particles, the tips of all pressure

taps are covered with a fine mesh wire gauze. U-tube glass manometers (5) were used to obtain the static pressure measures.

2.5. Procedure

For the fluid-dinamyc analyzes a bed consisting of inert material (quartz sand) with a reference mass of 8.5 kg was used, corresponding to a static bed with a height of 200 mm for all the experiments. Before introducing the quartz sand into the reactor, between 170 g and 1.275 kg of biomass (bagasse of each size fractions obtained) was mixed and added to the quartz sand, which corresponded to mass fractions of biomass of 2–15% respectively. The biomass and quartz sand particles were mixed in different ways; the smaller particles were mixed with the quartz sand out of the installation and subsequently placed in the reactor. The larger particles were placed in layers, initially a layer of quartz sand of 0.01 m in height and then one layer of biomass was placed and so forth.

The balance used to determine the fractions was the mark C&F model C15 with a maximum capacity of 15 kg and an accuracy of 1 g. All tests were performed at room temperature and atmospheric pressure (300 K and 100 kPa) respectively and they were analyzed qualitatively and quantitatively, evaluating parameters such as total pressure drop through the bed, the bed expansion and elutriation velocity of the particles. Visual observations and records of images were made by a digital camera. The experimental results were compared with the predictions of the reported correlations in the literature available. The comparison criteria used to validate the results was the Relative Mean Absolute Error (*RMAE*) defined as:

$$RMAE = \frac{\left|V_{mfe} - V_{mft}\right|}{V_{mfe}} \cdot 100 \quad \% \tag{14}$$

3. Results and discussion

3.1. Minimum fluidization velocity (V_{mf}) for mixtures of sugarcane bagasse particles and quartz sand

In this case the (V_{mf}) values were determined according to the method reported by Formisani et al. [44], using mixtures of sugarcane bagasse and quartz sand particles with a little segregation. Fig. 3 shows the behavior of pressure drop as function of the superficial velocity of air for a mixture of 2% of weight fraction of bagasse. With the increase of superficial velocity of the air, the total

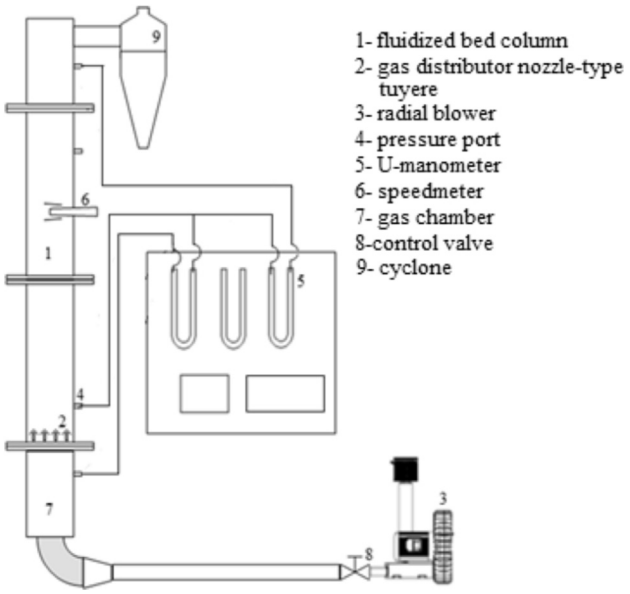

Fig. 2. Schematic diagram of the experimental installation.

pressure drop increases linearly in fixed bed until a determined point (V_{if}), defined as an incipient fluidization velocity. After pointing (V_{if}) the slope of the curve has a slight variation, but with the general trend of increase, as the superficial air velocity increases, reaching the point (V_{cf}). A pressure drop virtually constant determines the fluidization velocity and the state of a completely fluidized bed. This behavior is typical of binary systems composed by particles with different sizes and densities. It makes possible to differentiate two monodisperse systems because a minimum fluidization occurs in a range between (V_{if}) and (V_{cf}) [45].

In Fig. 4, the fluid-dynamic behavior of mixtures of sugarcane bagasse particles and quartz sand is shown through a sequence of photos. In this case the bed was assembled in layers, being the lower layer of quartz sand, subsequently one layer of bagasse up and another quartz sand layer. At low air velocities the bagasse particles remain immobile. When the superficial air velocity is near the (V_{if}), it is observed that the quartz sand (*jetsam particle*) of the upper part, at some point, begins to fluidize, due to the formation of preference channels in the bed where the velocity of the gas exerts a sufficient drag force to move these particles. An increase in the superficial velocity of the gas brings as a consequence the

Table 3
Correlations for determination the minimum fluidization velocity for binary mixtures.

Author	Correlation	Auxiliary equations
Zhong et al. [7]	For $\rho_{pm} > 1000 V_{mf} = 0.00145\left[\frac{d_{pm}^{2}\cdot(\rho_{pm}-\rho_g)}{\mu_g}\cdot\left(\frac{\rho_{pm}}{\rho_g}\right)^{1.23}\right]^{0.363}$ For $0 < \rho_{pm} < 1000 V_{mf} = 0.00012\left[\frac{d_{pm}^{2}\cdot(\rho_{pm}-\rho_g)}{\mu_g}\cdot\left(\frac{\rho_{pm}}{\rho_g}\right)^{1.23}\right]^{0.633}$	$\rho_{pm} = \frac{X_{in}\rho_{in}+X_b\rho_b}{X_{in}+X_b} d_{pm} = d_{p1}\left[\left(\frac{\rho_1}{\rho_2}\right)\left(\frac{d_{p1}}{d_{p2}}\right)\right]^{\frac{m_2}{m1}}$ Where: d_{p1} is the particle diameter with smaller weight fraction in the mixture, no matter if it is a biomass or an inert material
Paudel & Feng [8]	$R_{emf} = \left\{\begin{bmatrix}30.28^2+\\ 0.046(1-X_b)+\\ 0.108X_b^{0.5}\end{bmatrix} A_{rm}\right\}^{0.5} - 30.28$	A_{rm} as defined by Goossens et al. [35]
Rao & Bheemarasetti [17]	$V_{mf} = \frac{d_{pm}^{2}(\rho_{pm}-\rho_g)\cdot g}{1650\mu_g}$ Para $R_{emf} < 20$	$d_{pm} = k\left\{d_{in}\left[\left(\frac{\rho_{in}}{\rho_b}\right)\left(\frac{d_{pb}}{d_{pi}}\right)\right]^{\frac{X_b}{X_{in}}}\right\}\rho_{pm} = k\frac{X_{in}\rho_{in}+X_b\rho_b}{X_{in}+X_b}k = 20\cdot d_{pin} + 0,36$
Si and Guo [23]	$R_{emf} = \sqrt{C_1^{2} + C_2\cdot Ar_m} - C_1$	$C_1 = 25.65\cdot(\phi_b^{0.21}\cdot\phi_{in}^{0.15}) C_2 = 0.056\cdot(\phi_b^{-0.045}\cdot\phi_{in}^{0.025})$

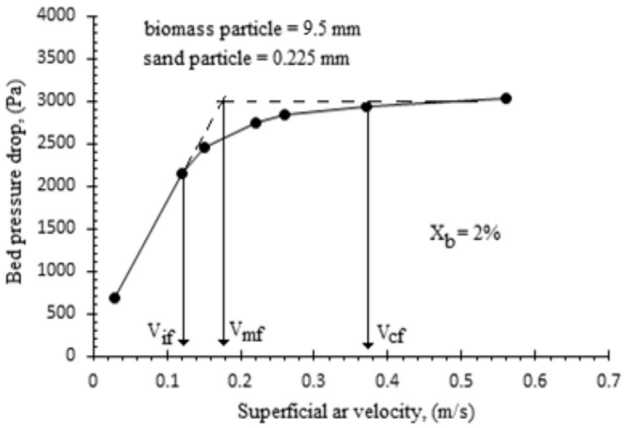

Fig. 3. Pressure drop as function of superficial air velocity for mixtures of sugarcane bagasse and sand particles.

emergence of small bubbles in the quartz sand layer at the bottom of the bed above the distributor. The quartz sand particles migrate to the top layer of biomass particles behaving as (*flotsam*). Subsequently a further increase in the superficial air velocity, results in the bed expansion, breaking the interparticle forces (liaison and cohesion forces) by the interaction and collisions with the quartz sand particles, stirring and mixing the entire bed. Thus, at (V_{cf}), the bed remains in the fluidized state causing the pressure drop remains substantially constant. After (V_{cf}), the bed achieves a better state of fluidization, perceiving a good mix and circulation of particles. This behavior was observed in the fluidization of mixtures of quartz sand and sugarcane bagasse particles with mean diameters between 9.5 and 0.72 mm, which represents a ratio biomass/sand between 42.2 and 3.2 respectively. Being different from the one reported by Zhang et al. [46], with biomass/sand ratio of 10, where the authors observed a slight contraction of the fixed bed where the superficial gas velocity was near the (V_{if}). This fact may be motivated by the initial arrangement of the bed (the experiment was starting from well-mixed packing) and the geometry of the experimental installation. The physical properties of the biomass particles used in each case can also affect the bed fluid- dynamic.

Also, the behavior reported in this study differs from that reported by Rao and Curtis [47], for very large ratio size particles where the *jetsam* particles remain immobile in the bed, being the *flotsam* particles the ones that first begin to fluidize as superficial air velocity is increased. This difference can be motivated by the fact that both types of particles used in this study could be considered practically spherical ($\phi = 0.9$) and, although they have differences of diameters, there density is practically the same. This is the reason why the smaller particles can be expected to have a tendency to fluidize first due to the fact that they percolate across the interspaces among larger particles, behaving as *flotsam*, which has been well established in different studies [48–51]. Very different from systems that use polydisperse biomass particles, such as sugar cane bagasse with extreme characteristics of size, density and sphericity that tend to intertwine and interlock with each other forming a kind of network with a high porosity, allowing the smallest particles, although higher density, pass through these spaces and fluidize first.

As the diameters of the bagasse particles were decreasing in the binary mixture, the fluidization diagram shown in Fig. 3 was changing. Many peaks were observed in the pressure drop profile with ups and downs, similar to the blades of a handsaw. According to Rao and Curtis [47], these peaks are features of binary systems with a big difference in size and can be explained by the phenomena called entrapment.

With the increasing of the superficial velocity of the gas, the pressure drop in the bed is also increased up to a given value where the bagasse particles retained by the sand particles start to fluidize. When the sand particles reach the surface of the bed, they return to the end of the column as they are a little denser, catching and retaining the rest of the biomass particles in the lower layers. This phenomenon is associated to the first peak observed in the profile of the pressure drop.

After the first peak, the pressure drop is once again increased due to the velocity until the second layer of bagasse particles migrates to the surface of the bed. Thus, as the bagasse particles migrates to the surface of the bed, many peaks are being observed in the profile of the pressure drop until a value of the superficial velocity of the gas is reached, where the pressure drop remains almost constant, defining the state where the whole bed is fluidized (see Fig. 5).

In this study, this phenomenon was observed in mixtures of bagasse particles with diameters between 3.55 and 0.445 mm and quartz sand with a mean diameter of 0.225 mm, in both case: for a well-mixed binary system and for a segregated binary system. Which differs from the studies by Rao and Curtis [47] and Formisani et al. [51], where this phenomenon was only observed in well-mixed binary system.

This difference in their behavior perhaps can be explained by the type of particles used in each study. In our case, the sugarcane bagasse particles differ, to a great extent, to sand particles, not only in their characteristic diameters, but also in their density with a diameter ratio biomass/sand between 2 and 42 and a density ratio sand/biomass between 4.9 and 5.5, being the biomass particles the biggest, but the lightest.

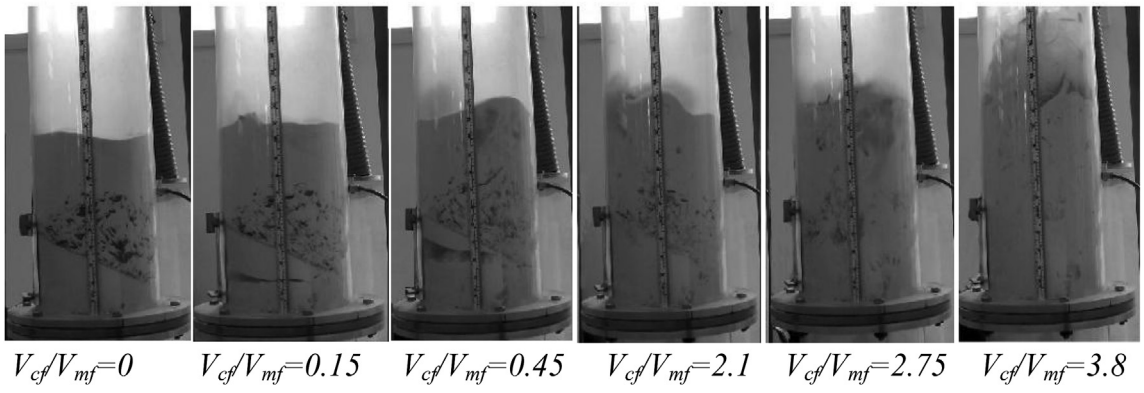

Fig. 4. Fluidization behavior of binary mixtures bagasse/quartz sand (d_{pb} = 7.125 mm, X_b = 2%).

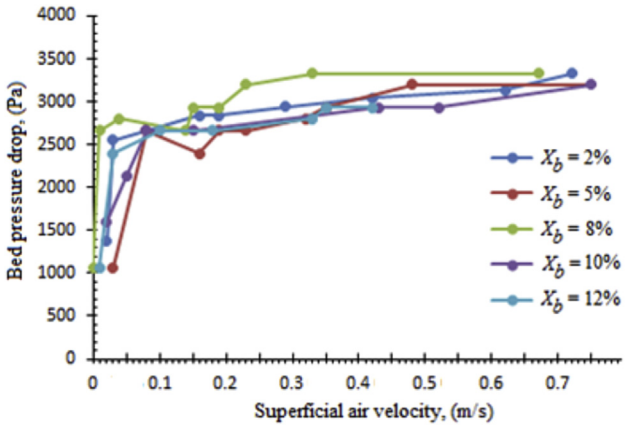

Fig. 5. Bed pressure drop vs superficial air velocity for mixtures of bagasse with mean diameter of 0.445 mm and quartz sand of 0.225 mm.

3.1.1. *Influence of the increase of the biomass fraction and the ratio of the biomass to the column diameter in the (V_{mf})*

Table 4 and Fig. 5 show that (V_{mf}) has a tendency to increase as the fraction of mass of bagasse in the mixture (X_b) increases. The same behavior has been reported by other researchers such as Zhong. al. [7] and Rao and Bheemarasetti [17], using other types of biomass. The possible reason for this typical trend may be due to the increased porosity of the bed to the level that increases the average diameter or the mass percentage of the biomass particles in the mixture because the mass of the inert material in the bed is constant, but the bed height is variable. In the case of mixtures of bagasse and quartz sand particles, this behavior takes place in the range of diameter of 3.55–0.445 mm, where an increase of any of the two mentioned parameters will result in an increase of the effective mean diameter of the mixture. V_{mf} increases with higher biomass fraction (X_b) although the decrease of the effective average density should cause a decrease of (V_{mf}). This reveals, in this case, that the influence of the characteristic diameter of the particles in the mixture prevails in the fluid-dynamic behavior of these materials.

Table 4
Experimental (V_{mf}) with different bed composition.

d_{pb} (mm)	X_b (%)	d_{pm} (cm)	ρ_{pm} (g/cm^3)	V_{mf} (m/s)
9.500	2	0.025	2.369	0.31 ± 0.03
7.125	2	0.025	2.372	0.20 ± 0.02
3.555	2	0.025	2.376	0.18 ± 0.03
	5	0.028	2.118	0.42 ± 0.04
1.770	2	0.024	2.378	0.17 ± 0.01
	5	0.027	2.123	0.42 ± 0.01
0.885	2	0.024	2.387	0.16 ± 0.007
	5	0.026	2.141	0.17 ± 0.030
	6	0.027	2.070	0.18 ± 0.007
	7	0.027	2.003	0.40 ± 0.020
	8	0.028	1.941	0.72 ± 0.030
0.722	2	0.024	2.379	0.17 ± 0.03
	5	0.027	2.124	0.32 ± 0.02
0.445	2	0.023	2.395	0.16 ± 0.02
	5	0.024	2.157	0.17 ± 0.01
	8	0.024	1.962	0.19 ± 0.01
	10	0.025	1.850	0.20 ± 0.01
	12	0.025	1.751	0.25 ± 0.02
0.225	2	0.022	2.411	0.06 ± 0.007
	5	0.020	2.189	0.07 ± 0.004
	10	0.019	1.898	0.07 ± 0.007
	15	0.018	1.676	0.06 ± 0.010
0.075	2	0.019	2.426	0.030 ± 0.007
	5	0.016	2.221	0.035 ± 0.007
	9	0.014	1.997	0.030 ± 0.005

For binary mixtures containing very small bagasse particles, with mean diameter smaller or equal to the quartz sand ($0 < d_{pb} \leq 0.225$) (Table 4), it is observed that the (V_{mf}) tends to remain fairly constant or decreases when the mass fraction of biomass is increased. This is due to the effective average diameter of the mixing decreases as the ratio biomass/sand ($d_{pb}/d_{pin} \leq 1$) decreases, as well as the amount of bagasse increases in the binary mixture (X_b). However, other fluid-dynamic parameters as the bed pressure drop (ΔP) and complete fluidization velocity (V_{cf}) remain almost constant with the increase of the bagasse fraction (X_b), being approximately 2.7 kPa and 0.03 m/s respectively. Rao and Reddy [13] reported a similar situation in the behavior of the minimum fluidization velocity in mixtures of biomass and sands with different sizes, as well as studies carried out by other researchers using more conventional particles [51,52].

Considering the relationship between the characteristic diameter of the biomass particles (bagasse) and the diameter of the fluidization column (D_c = 190 mm) an increase of (V_{mf}) was corroborated as the mean diameter of the biomass particles increased. This is similar to that reported by Chok et al. [52] using four different sand types. However, the reason of the increase of this velocity has different explanations. In the study by Chok et al. [52] this fact can be explained because an increase in the diameter of the particles is going to lead to an increase in their weight and therefore to an increase in the buoyancy force necessary to fluidize them, considering that the apparent density is the same for all types of sand used, so it can be said that the hydrodynamic forces (gas - particle interaction) will have a prevalence in relation to interparticular forces (particle - particle interaction). In our case the explanation would be a little there different, mainly due to the use of biomass particles with low sphericity and density but with high cohesive forces, factors that will influence the formation of preferential channels in the bed [53]. As the bagasse particles increase in diameter, the length also increases, having a bigger tendency to cross-link with each other, forming strong bonds, on the other hand, sphericity decreases, which causes bigger voids between them, whereby the smaller particles of sand can easily pass through by decreasing the contact area and collisions in particle-particle interactions [54], thus higher surface velocities of the gas must be used to break those high interparticular forces may be as the result of Van der Waals, electrostatic, capillary and viscous forces [55].

In regards to the influence of the bed aspect ratio H/D on the (V_{mf}), it was observed that in the range of biomass particle diameters between $0 < d_{pb} \leq 0.225$ mm, where this parameter varied between 1.3 and 3.3 (Table 5) and the mixture had a high tendency to segregation by density difference, for all conditions of mass fractions tested, H/D differences did not significantly influence the value of (V_{mf}), remaining practically constant and coinciding with the study reported by Ref. [45]. However; in the range of bigger diameters 3.555–0.445 mm, where the mixture was more prone to segregation due to the difference of mean diameters, a significant increase in (V_{mf}) was observed with the increase of the mass fraction of bagasse and, consequently, with the increase of bed aspect ratio H/D between 1.3 and 2.85. This fact made it different from the one observed by Ref. [45]. One possible explanation, in this case, would be the extreme differences between the types of particles used in each case, where binary mixtures using biomass particles will have a very different behavior from conventional particle mixtures due to their low sphericity, density and high cohesive forces.

The measures showed a very similar typical trend, where (V_{mf}) is not related to a single point, but within the interval (V_{if}) and (V_{cf}), characterizing the different regimes of fluidization. Table 4 showed the experimental results of an average of two observations of fluid-

dynamic behavior of mixtures of sugarcane bagasse particles with different mean diameters and quartz sand.

3.2. Mixing and segregation

During the experimental process, the mixing and segregation of particles can clearly be observed. By visual observation, anyone can better understand the mixing and segregation mechanism.

The segregating phenomenon was observed in all the experiments of fluidizing mixtures of different diameters of bagasse and quartz sand particles expressing in a greater or less degree (Table 5), depending on the effective average diameter and the mass fraction of bagasse in the mixture.

It is observed in Fig. 5 that after the point (V_{if}), the pressure drop in the bed decreases slightly; this happens because in this value of superficial air velocity, the smaller particles (quartz sand particles) start to move among the spaces and holes left by the biomass particles, which remain static, not being observed yet the appearance of bubbles in the bed. An increase in the superficial air velocity may cause an increase the pressure drop, so that the bed increases again to a value similar to the weight of particles in the mixture per unit of area of the bed, remaining almost constant. At this point, it is considered that the larger particles (biomass particles) begin to move at the same time in which the first bubbles appear in the bed. Thus, a small portion of these bagasse particles begins to segregate at the top of the bed, behaving as *flotsam* and the quartz sand as *jetsam* [12], because the bagasse particles have a lower density than the quartz sand particles. A further increase in the superficial gas velocity will cause an increase in the flow and frequency of bubbles, which coalesce, increasing in size, as they go up the bed and enter into the bubbling regime, reaching a fully mixed and homogeneous bed. Fig. 6 shows this behavior in mixtures with 2% of weight fraction of bagasse particles with mean diameter between 9.5 and 0.445 mm. The ratio between the complete fluidization velocity and the minimum fluidization velocity to achieve a complete mixing was between V_{cf}/V_{mf} = 1.4–4.0; the highest values correspond to particles with bigger mean diameters.

Particles with average diameters between 3.55 and 1.77 mm presented the smallest ratios of V_{cf}/V_{mf} with values between 1.43 and 1.55 respectively, being this range where segregation occurred with less intensity.

This behavior is similar to that reported by Olivieri et al. [52] (System 1), where the bigger and less dense particles behave as *flotsam*, while the smaller and denser particles are segregated at the bottom of the bed as *jetsam*. Another study reported by Zhang et al. [46], specifically for biomass particles (cotton stalk), also shows this same behavior by defining three fundamental mechanisms for the emerging of segregation in the state of incipient fluidization: percolation effect -induced segregation, buoyancy force -induced segregation and bubble motion -induced segregation.

Theoretically, in binary mixtures with very large size ratio particles, the segregation phenomenon will have a tendency to decrease as the surface velocity of the gas is increased to a certain value, from which, it will have an inversion, tending to increase again [46,47]. However, what was visually observed during the experiments carried out in this study was a progressive tendency to decrease the segregation as the surface velocity of the gas was increased until its disappearance at velocities equal to or bigger than (V_{cf}), which is a more similar behavior to that reported in the study by Rao and Curtis [47] (Type B mixture). Therefore, it can be concluded that, at these velocities, the bubbles help a better mixing and homogenization of the bed [46,52]. In mixtures composed of diameters of biomass particles between $0.445 > d_{pb} \geq 0.075$ mm, whose component density ratio is equal to 4.9–4.3 respectively, the behavior of the segregation phenomenon manifested itself in a totally different way to the previously reported for the range of diameters $9.5 \geq d_{pb} \geq 0.445$ mm either for well-mixed beds and or for fully segregated beds.

In the particles with small diameter ratio biomass/quartz sand (1.0–0.3) was observed a severe segregation for superficial air velocities just above the (V_{mf}). In this occasion, the less dense biomass particles were the first to start moving in a bubble-free bed, being

Table 5
Details of mixtures and their properties.

Mixtures				Size ratio	Density ratio	H/D ratio	V_{cf}/V_{mf} ratio
Bagasse diameter	Mass fraction (%)	Jetsam	Flotsam	d_{pb}/d_{pin}	ρ_{in}/ρ_b		
9.500	2	sand	bagasse	42.2	5.54	1.30	4.03
7.125	2	sand	bagasse	31.7	5.49	1.30	2.75
3.555	2	sand	bagasse	15.8	5.40	1.30	1.43
	5	sand/bagasse	sand/bagasse			1.78	4.23
1.770	2	sand	bagasse	7.86	5.34	1.30	1.55
	5	sand/bagasse	sand/bagasse			1.65	4.19
0.885	2	sand	bagasse			1.33	2.75
	5	sand	bagasse			1.52	4.41
	6	sand	bagasse	3.93	5.14	1.77	6.94
	7	sand	bagasse			2.03	3.90[a]
	8	sand	bagasse			2.03	3.23[a]
0.722	2	sand	bagasse	3.2	5.33	1.30	2.08
	5	sand	bagasse			1.62	4.68[a]
0.445	2	sand	bagasse			1.33	2.62
	5	sand	bagasse			1.72	2.82[a]
	8	sand	bagasse	1.97	4.97	2.15	2.63[a]
	10	sand	bagasse			2.66	2.60[a]
	12	sand	bagasse			2.85	1.40[a]
0.225	2	sand	bagasse			1.30	2.66[a]
	5	sand	bagasse	1	4.61	1.77	3.28[a]
	10	sand	bagasse			2.54	4.14[a]
	15	sand	bagasse			3.30	6.83[a]
0.075	2	sand	bagasse			1.30	2.33[a]
	5	sand	bagasse	0.33	4.27	1.65	4.28[a]
	9	sand	bagasse			2.15	5.00[a]

[a] A small line that is not mixed begins to be observed in the surface of the unmixed biomass bed.

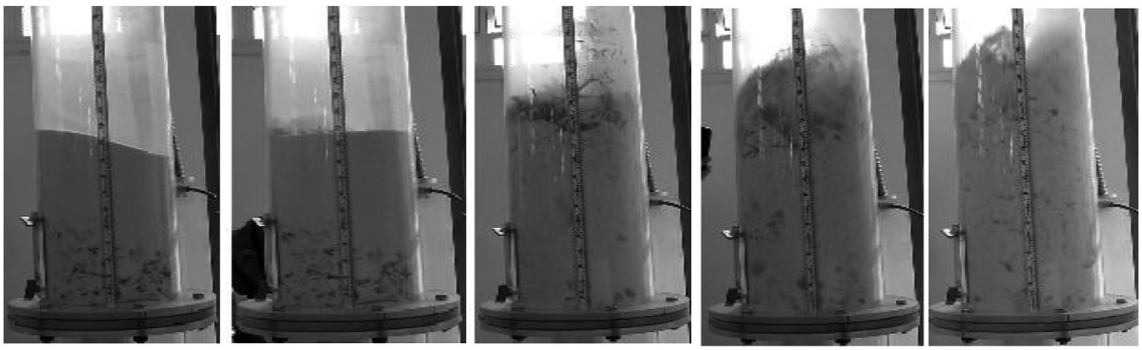

Fig. 6. Segregation phenomenon in mixture of bagasse/sand particles. (d_{pb} = 7.125 mm, X_b = 2%).

the sand particles maintained in the fixed state, as a result of the phenomenon of percolation, accumulating the biomass particles on the bed surface. An increase in the surface velocity of the gas promotes the emerging of the first bubbles in the bed, increasing the degree of segregation, observing two well-defined lines, an upper one composed by the *flotsam* particles and a lower one composed by the *jetsam* particles, both fluidizing separately. A subsequent increase in the surface velocity of the gas increases the frequency and size of the bubbles, which explode by reaching the surface, thus propelling the biomass particles to the freeboard. The downward motion of sand near the walls of the column and on the surface of the bubbles drags part of the biomass particles into the dense bed. This movement promotes a certain degree of mixing, but in a very incipient way, not reaching a good mixing and homogenization of the bed. Even when is used a high ratios of V_{cf}/V_{mf} = 5, was impossible achieves the completed mix the bed, and was observed a well- defined line of *flotsam* particles fluidizing at the surface. This result coincides with the results reported by Rao and Curtis [47] (Type E mixtures) where the segregation index decreases as velocity increases. Bigger values of the surface velocity of the gas causes the elutriation of the biomass particles of the bed.

The behavior explained above coincides with the studies of Olivieri et al. [52], Formisani et al. [51] and Formisani et al. [56], where particles with different densities and practically the same size (diameter) were used. In the first study the authors refer to a "fluidized-fluidized" segregation pattern: with a lower layer composed of *jetsam* particles and an upper one composed of *flotsam*, both in the fluidized state, equal to that observed in this study. In the second and third study, the two solids used in the mixture were quickly separated into two well-defined layers when the density ratio exceeded the value of three, differing in the fact that at higher surface velocity, they achieved the state of mixing, something that was not possible in this study; however, they argued that there is no defined mixing velocity for all density-segregating mixtures.

From the observations made in this study, it can be concluded that mixtures using particles with very different properties of size, shape and density as used in this study are quite difficult to mix. As the size ratio decreases ($d_{pb}/d_{pin} \leq 1$), the mixtures of both types of particles become even more difficult to mix, being almost practically impossible to achieve a well-mixed bed in all conditions tested. In most cases bagasse will behave as *flotsam* because the bulk density of the mixtures is always bigger than that of the bulk density of bagasse particles, which is in line with the study reported by Rasul et al. [55].

3.2.1. Influence of the increase of the biomass fraction in the segregation degree

Fig. 7 shows the effect of increasing mass fraction of sugarcane bagasse in the mixture on the segregation. It can be seen that an increase in biomass fraction of the mixture (X_b) from 2% to 5% increases the intensity of the bed segregation when using bagasse particles with mean diameter ≥ 1.77 mm (diameter ratio biomass/quartz sand $d_{pb}/d_{pin} \geq 8$). V_{mf} increases because the fine bagasse particles tend to become entangled, forming a network with a high cohesive force which must be broken to achieve fluidization. This interlacement of biomass particles mixed with sand has been reported in previous studies by Pilar et al. [18] and Chok et al. [19], using other types of biomass with physical characteristics very similar to those of the sugarcane bagasse particles.

The increase of the weight fraction of bagasse particles in the mixture in the range of $0.885 < d_{pb} \leq 9.5$ mm will increase the likelihood of interlacement and cohesion of the particles and, as a result, higher superficial air velocities are required not only to overcome the gravitational force, but also to break these links and to ensure the fluidization of the bed. In the case of binary mixtures with X_b = 5%, using bagasse particles with average diameters between 1.77 and 3.55 mm (d_{pb}/d_{pin} = 8 - 15) the (V_{cf}) was between 1.76 and 1.78 m/s respectively, observing a phenomena called reverse segregation.

The reverse segregation occurs or is expected when there is an inversion in the layers occupied by the particles of *jetsam* and

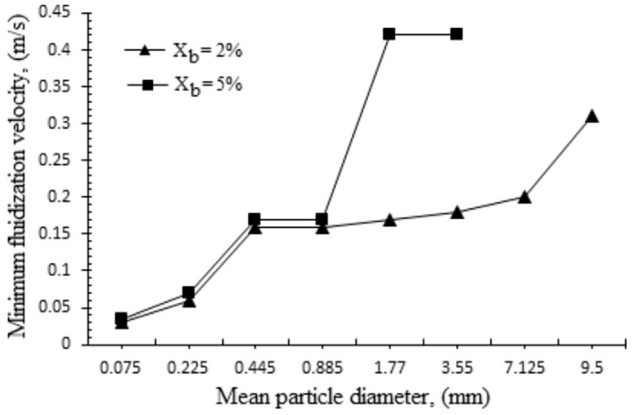

Fig. 7. Influence of mass fraction in segregation.

flotsam respectively [57] and [58]. At a low surface velocity of the gas the sand particles began to percolate through the spaces left between the biomass particles towards the surface of the bed, where a thin fluidized layer was created, where the biomass was in the fixed bed state without any movement. As the surface velocity of the gas increased, a bigger amount of sand was transported, creating an increasingly thick layer on the surface of the bed. Progressive increases in velocities led to the appearance of the slugging flow with slight vibrations of the bed which favored, together with the particle - particle interaction, the strong bonds of the cohesive forces and cross - links of the biomass particles to be broken, bringing about some degree of mixing. The increase of the bubbles in the bed favored the bigger and less dense particles to start to be dragged by the wake to the surface of the bed, visualizing the phenomenon of segregation due to the bubbles previously explained and it showed the inversion of the layers of the particles, where the less dense and bigger particles that at first behaved as *jetsam* and remained at the bottom of the bed, were subsequently observed on the bed surface, behaving as a *flotsam*.

Although high surface velocities of the gas were used, a homogeneous mixture of the bed was not observed. A practically pure layer of sand was visible near the distributor. A mixture region was created on the layer where biomass and sand particles were well mixed occupying almost half of the bed, with a thin layer of biomass pure particles that was gaining space, until the three regions were clearly established: pure practitioner *jetsam* fluidizing in the lower region near the distributor, *jetsam* and *flotsam* mixed in the central part of the bed and a thin layer of *flotsam* on the surface of the bed that was not possible to mix even if high surface velocities of the gas were used. This behavior was observed for mixtures composed by bagasse particles with a mass fraction of 5% and average diameters between $1.77 \leq d_{pb} \leq 3.55$ mm. Binary mixtures using larger particle diameters $3.55 < d_{pb} \leq 9.55$ mm (20–40 times higher than the quartz sand) initially showed the same behavior, with the difference that the biomass particles remained segregated and practically static in the bottom of the bed, functioning as if they were a porous plate where the sand was fluidized on their top. Even using high superficial gas velocities (>2 m/s), the bed remains totally segregated, being impossible to fluidize it.

Through a series of photos of the bed, Fig. 8 shows the segregation for $X_b = 5\%$, where an inversion of the segregation phenomenon occurs. In this case, the bagasse particles remain in the bottom of the bed without being fluidized, while the fluidized quartz sand remain on the top, the bagasse behaves as *jetsam* and quartz sand as *flotsam*. This phenomenon takes place in binary mixtures using bagasse particles with a mean diameter ≥1.77 mm, as for the bagasse in its natural form to $X_b > 5\%$.

The increase in the mass fraction above 2% of bagasse particles with mean diameters between $0.885 \geq d_{pb} \geq 0.075$ mm in the binary mixture causes an increase in the trend towards the emerging of segregation (Fig. 9), when the contrary would have been expected [12,51]. In shallow beds there is a high number of small bubbles disturbing the bed that allow an easy segregation of the jetsam particles, whereas in deep beds with a high H/D ratio, the bubble frequency decreases as height increases, which causes a minor perturbation, decreasing the tendency to a segregation of the particles [12]. These facts are relatively true, since as explained above, at first the emergence of bubbles promotes the appearance of the phenomenon of segregation. With the increase of the superficial velocity of the gas to certain values, the bubbles can help more in the remixing of the bed, favoring, in a certain degree, the mixing of the particles rather than the appearance of segregation [46,52]. In binary mixtures using bagasse particles with mean diameter $d_{pb} = 0.885$ mm, the limit for a good mixing in the bed was up to 6% of mass fraction of bagasse. Higher fractions cause a thin layer of biomass particles (flotsam) on the surface of a bed. In binary mixtures using smaller bagasse diameters $d_{pb} \leq 0.445$ mm this phenomenon occurs earlier (5% mass fraction of bagasse), which can be explained by the difference in the thrust forces experienced in each size range, since the smaller particles have a higher bulk density, requiring a bigger buoyancy force to reach the fluidization [46].

It was worth noting that in none of the experiments performed in this range of particle diameters, the phenomenon of inverse segregation was observed. Even if the bed is totally segregated, it is possible to be fluidized, due to the fact that the bagasse particles in the size range of $0.445 \geq d_{pb} \geq 0$ mm are able to be fluidized without the addition of inert materials, which has been discussed in another work, keeping bagasse as *flotsam* and the sand as a *jetsam* in two well-defined layers.

An increase in the superficial gas velocity, to promote mixing of both components, brings about the elutriation of large amounts of bagasse particles from the bed into the freeboard, representing a decrease in the residence time and low efficiency in combustion or gasification processes in practical applications. Thus, it can be concluded that the bagasse particles with a mean diameter of 0.885 mm, mixed with quartz sand are the ones that show the best

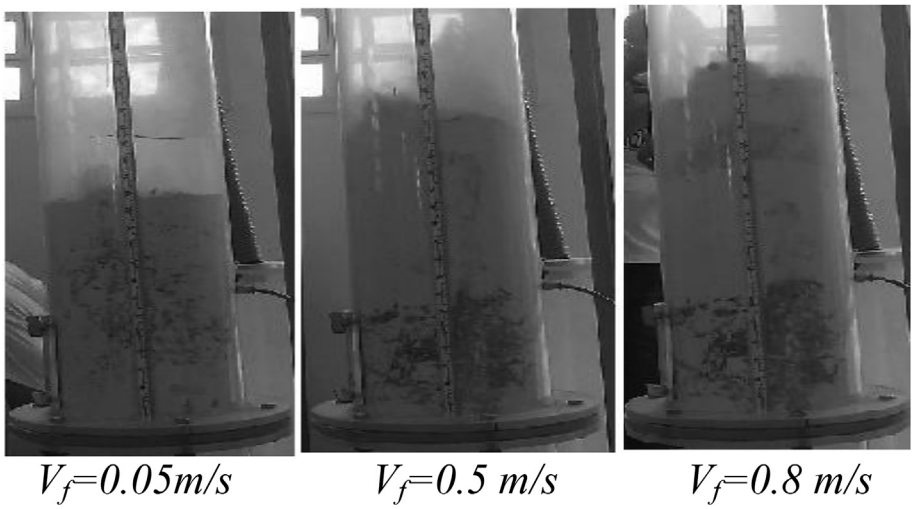

Fig. 8. Inverse segregation in mixtures of bagasse/quartz sand particles. (d_{pb} = 9.5 mm, X_b = 5%).

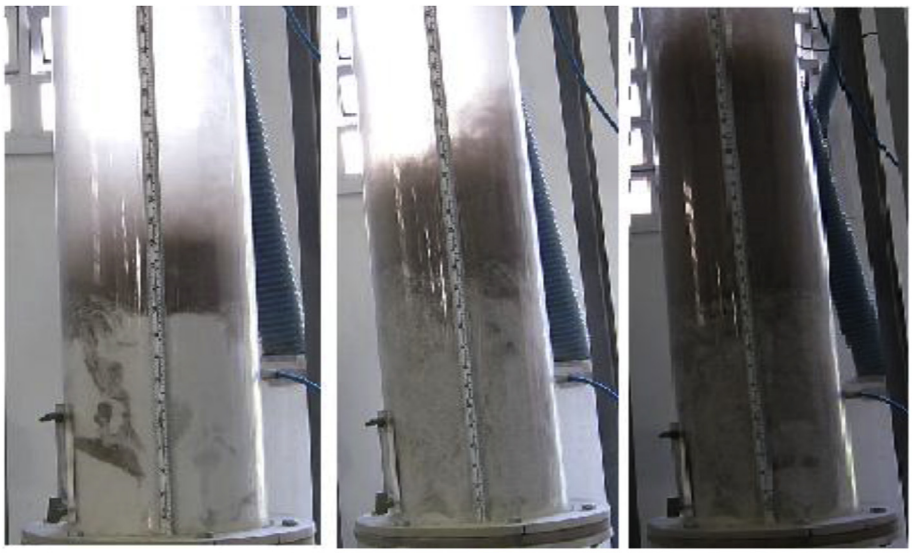

Fig. 9. Segregation in mixtures with fine particles of bagasse. (d_{pb} = *0.225 mm*).

fluid-dynamic behavior when it increases the fraction of bagasse mass above 5%, coinciding with the study reported by Pérez et al. [60].

Bagasse particles with extreme forms, low density and different sizes, are very difficult to fluidize without the addition of an inert material that favor particle-particle interaction because de bagasse particles have the tendency to "hook up" each other, forming even bigger chunk of particles, as if it were a network that must be broken in order to attain or sustain fluidization [54]. The addition of sand has been demonstrated to be an effective solution to this problem. But the use of sand in the mixtures is not a guarantee to achieve a good fluidization. Much attention should be paid to the conditions and nature of the mixtures to avoid problems in fluidization. The results obtained in this study, are recommended for sugarcane bagasse in its natural form, with maximum mixtures between 2 and 3% of mass fraction to achieve a good fluidization and promote a homogeneous mixture of the bed. Great quantity of biomass can cause problems in the fluid-dynamic behavior such as the appearance of an intense segregation in the bed, which do not allow the fluidization of mixtures with above 5% of weigh fraction of bagasse particles. These results are in agreement with the study reported by Sharma et al. [11].

3.3. Prediction of minimum fluidization velocity for mixtures of sugarcane bagasse and quartz sand

Fig. 10 shows the results obtained in the theoretical and experimental evaluation of (V_{mf}) of mixtures of sugarcane bagasse particles and quartz sand with 2% mass fraction of bagasse (X_b = 2%). Virtually none of correlations reported before, can describe the behavior of (V_{mf}) of mixtures of bagasse particles and quartz sand. Most of these models were developed for binary systems (biomass/sand) with different physical characteristics to bagasse, but they are the most widely used today by many researchers [61,62] because they permit the fluid-dynamics modeling and project of bubbling fluidized bed reactor [63,64]. Correlations of Rao and Bheemarasetti [17], Ergun [33] and Wen and Yu [31] got to predict only one of the eight mixture compositions tested experimentally with mean errors of 9%, 7% and 40% respectively, being suitable only for mixtures with very small bagasse particles (d_{pb}=0.075 mm). For the rest of the mixtures the reported errors pass 50% of the experimental value. Likewise the correlation reported by Si and Gou [23] also predicted the (V_{mf}) within 40% of deviation of the experimental values for only one mixture compositions. It showed a higher deviation for the rest of mixtures (>50%).

Also the correlation of Paudel and Feng [8] does not predict good results, being suitable only for mixtures that use bagasse particles with effective mean diameters smaller than 0.225 mm. The errors reported by this correlation were between 2 and 36% of the experimental value for the previous diameter range.

The only correlation reported in Table 3, which predicted reasonably the (V_{mf}) in mixtures of bagasse and quartz sand particles was the one reported by Zhong et al. [7] in the range of

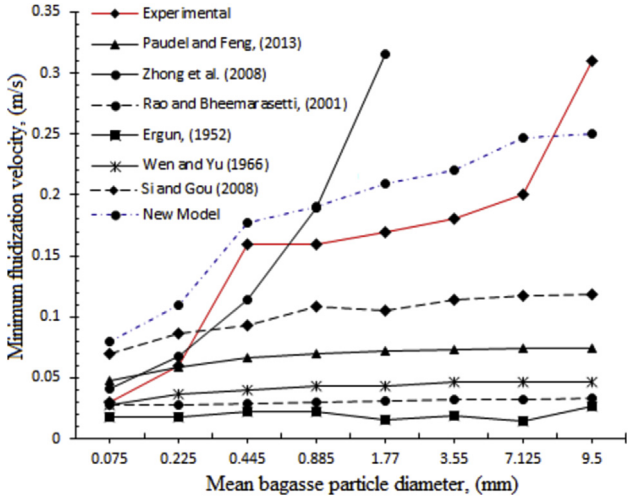

Fig. 10. Experimental and theoretical minimum fluidization velocity for mixtures of sugarcane bagasse and sand with X_b = 2%.

diameters from 0.885 to 0.075 mm, with means errors within 13–28%. When this correlation was evaluated in mixtures composed by bagasse particles with diameters greater than or equal to 1.77 mm, the errors were more than 80% of the experimental value. Overall results indicate that none of the available correlations [7,8,17,23,30,31] well predict the minimum fluidization velocity for the entire range of mixture compositions investigated in this study. The large error deviation between calculated and experimental values of (V_{mf}) can be influenced by the conditions in which these correlations were developed and the type of particles used for its determination. Specifically in the case of the correlations of Paudel and Feng [8] and Rao and Bheemarasetti [17] that have been developed for biomass, such differences may be motivated by the fact that in these studies the authors have developed their models in terms of the biomass fraction mixed with sand, without allowing the influence of the diameter and irregular shape of the particles, especially for long and thin biomass with size, ratios and density between the biomass and the inert material (quartz sand) which are very large, influencing the segregation and fluid-dynamic behavior of mixtures. In the specific case of the correlation of Zhong et al. [7], the differences may be due to the geometry of the fluidization column and to the differences in ratios of size and densities between the biomass and the inert materials used in each case [51,52]. In spite of changing the relationship between length and cross-sectional diameter of long and thin biomass particles ($1 < L/d_{pt} < 20$), the ratio of biomass particle size to inert material d_{pb}/d_{pin} mixture varies in a narrow range (0.32–10), contrary to what happens in this study where such ratio oscillates between 0.33 and 42.2. It is known that the differences in size and density of the particles that make up the mixture as well as the mass fraction of each component will influence the porosity of the bed, which is a key variable for the understanding of the gas-particle interaction in the emergence of segregation and, therefore, in the fluid dynamic behavior of the mixture [56,65], this together with other factors such as the sphericity of the biomass particles may be some of the causes of the failure of model of Zhong et al. [7], in the (V_{mf}) prediction for particles with mean diameters bigger than 1.77 mm.

Using the experimental values of (V_{mf}) determined in this work, it was possible to develop a new correlation by fluid-dynamic parameters such as Reynolds and Archimedes numbers, which take into account the use of binary mixtures of sugarcane bagasse and quartz sand particles, varying sizes, shapes, mixture compositions and densities. Using a nonlinear regression method, the value of the coefficient that fit the general expression for the correlation of binary mixtures were found with an $R^2 = 0.87$ and average standard deviation of ±0.016 m/s, allowing the determination of the minimum fluidization velocity more precisely than the previous correlations reported in the literature. The new proposal of correlation is presented below:

$$V_{mfmixture} = \frac{0,00002 \cdot A_{rm}{}^{1,7125} \cdot \mu_g}{d_{pm} \cdot \rho_g} \tag{15}$$

Fig. 11 shows a comparison between the experimental results of the (V_{mf}) and the results predicted by the correlation developed in this study and the previous correlations reported in the literature by determining Reynolds number according to equation (8). The correlation reported by Zhong et al. [7] predicts 12 of the 25 experimental conditions acceptably tested, with errors under 30%. Similarly, the correlation reported by Si and Gou [23] predicted only three of the twenty five mixture compositions with minor errors of 30%; approximately 32% of the predicted values with this correlation showed relative errors between 30 and 40% and 44% showed relative errors equal or bigger than 60%. Also the correlation reported by Paudel and Feng [8] presented higher relative errors of approximately twenty out of the twenty five mixture compositions. However; the new correlation developed in this work can predict 88% of the experimental conditions with errors minor or close to 30% of the experimental value, being proven a better precision and accuracy in the results predicted in regards to previous models. While errors of this magnitude might be considered big errors; in this case, they are considered to be an acceptable one because of the wide variability of tested conditions, considering that the models developed today have intrinsic errors of up to 34%, as in the correlation of Wen and Yu, which is the most commonly model used today [50].

Fig. 10 shows the behavior of the new correlation developed in the present work for a 2% of mass fraction of biomass in the mixture. It can be stated that the new correlation has a tendency to overestimate, in general, the value of (V_{mf}) for the entire size range of particles studied; being for particles bigger than 0.15 mm when the model has an acceptable behavior and errors less than 30% of the experimental value reported. However, for very small particles, smaller than 0.15 mm, the error is bigger than 30%. For the rest of the tested experimental conditions the model acceptably predicts

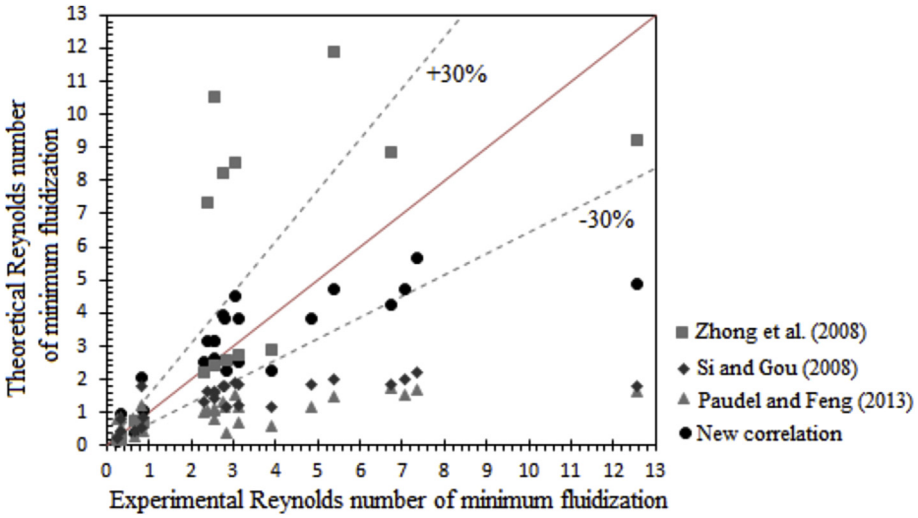

Fig. 11. Comparison of experimental (V_{mf}) with predicted data by the correlations of the present work and in the literature.

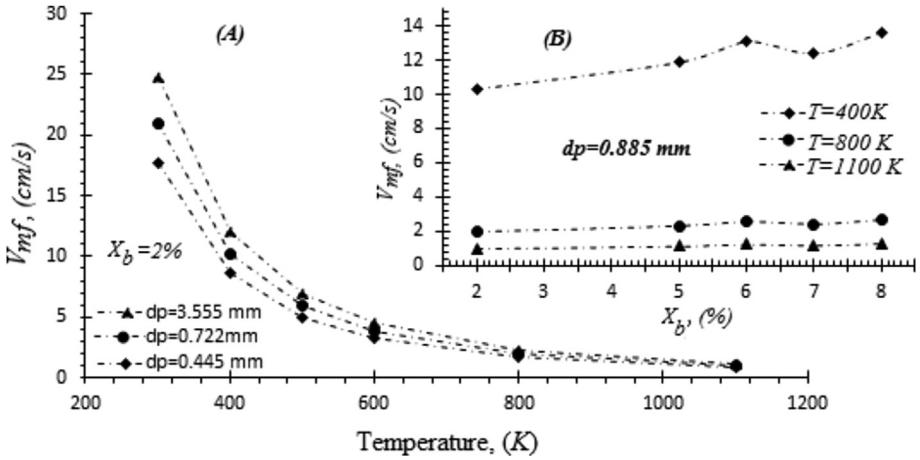

Fig. 12. Dependence of minimum fluidization velocity on temperature.

the value of the minimum fluidization velocity, showing smaller relative errors of 30% of the experimental value.

In spite of this new correlation, it was developed at environmental pressure and temperature conditions, as in most correlations reported in the literature, there is proven evidence that allows the application of the cold model in real operating facilities at high temperatures [67], through similarity relations applicable when the model obtained at room temperature and the installation working at high temperature have the same value of: Froude number, Reynolds number, solid to gas density ratios, sphericity and dimensionless particle size distributions. In addition, the two reactors must be geometrically similar, that is, all linear dimensions must be the same [68,69].

Fig. 12 (*A*) shows the behavior of the minimum fluidization velocity obtained with the new model, as a function of temperature and mean diameter in a mixture with a 2% mass fraction of bagasse particles. The trend in all cases is a decrease of the (V_{mf}) with the increase of temperature. In the range between 600 and 1100 K, the decrease is much less accentuated, reaching almost constant values, regardless the particle diameter of bagasse used in the mixture, in this region of high temperatures. The previous behavior is in agreement with the studies reported by Jiliang et al. [70] using different types of particles with a wide distribution of sizes and follows the trend of the studies developed by Formisani et al. [71] and Subramani et al. [72] which corroborate a decrease in (V_{mf}) with increasing temperature.

Fig. 12 (*B*) shows that V_{mf} decreases with increasing temperature using particles with mean diameter of 0.885 mm (V_{mf}) has a slight tendency to increase with the mass percentage of bagasse at 400 K, coinciding with the experimental results obtained at room temperature. At higher temperatures (800 K) this tendency is almost imperceptible, maintaining an almost constant (V_{mf}) value, without having the influence in this result of the increase in the mass fraction of bagasse particles in the mixture. This type of behavior is coherent, taking into account that in these high temperatures the devolatilization of the biomass particles takes place, resulting in the release of a volatile material that causes the emergence of *endogenous* bubbles [73], being the reason why the volumetric fraction of the bubbles has a tendency to increase strongly above 400 °C, causing an increase of the porosity in the emulsion phase and, consequently, a decrease in the velocity [74]. However, the increase in temperature also causes an increase in interparticular attraction forces, which would lead to an increase of (V_{mf}). These two types of opposite effects act together and balance each other, thus stabilizing the (V_{mf}) at high temperatures [70]. As for the segregation phenomenon, explained before, it is possible that it also can be manifested at high temperatures, according to the individual bubble segregation pattern detailed in the study by Bruni et al. [73].

4. Conclusions

In this work the fluid-dynamic behavior of particles of sugarcane bagasse with different diameters mixed with quartz sand in different mass fraction was experimentally studied and the minimum fluidization velocity in every case was determined. Considering the experimental results, some conclusions have been drawn:

1) The minimum fluidization velocity is not related to a single point, but to the interval between (V_{if}) and (V_{cf}), characterizing the different regimes of fluidization. For mixtures with diameter ratios biomass/sand between 2 and 42, and density ratios sand/biomass between 4.9 and 5.5, this parameter behaved in two different ways. In the range $9.5 \geq d_{pb} > 0.225$ mm, the (V_{mf}) increase as the diameter of the biomass particles increased, as well as with the increases the mass fraction of biomass. On the other hand, for binary mixtures with diameter ratio biomass/sand ≤ 1, the (V_{mf}) remain almost constant or even may show a slight decrease in fractions with X_b between 2 and 15%.
2) For sugarcane bagasse in its natural form, containing a mixture of particles of different sizes $0 < d_{pb} < 9.5$ mm and characteristic ratio length/particle diameters between $3.4 < L/dpb < 8$, the adequate mass fraction to obtain a good mixing and bed homogenization is 2%. Higher biomass fractions in the mixture can cause the emerging of channeling and segregation, due to the decrease in the bulk density of the mixture and the strong tendency of the bagasse particles to come together and intertwine each other, forming bigger voids between them. For $X_b >$ 5% it is impossible the fluidization of the mixture in the bed, observing the phenomenon of the reverse segregation.
3) A good fluidization regime (with low segregation) was obtained in the range of diameters of $0.445 < d_{pb} < 1.77$, with a ratio length/diameter of biomass particle between 6 and 7, and 2% of mass fraction of biomass in the mixture, corresponding to a ratio of diameters biomass/sand $2 \leq d_{pb}/dp_{in} \leq 8$. The best fluid-dynamic behavior was obtained for $d_{pb} = 0.885$ mm, observing a good performance in mixtures with up to 6% of mass fraction of bagasse particles, ($d_{pb}/d_{pin} \approx 4$).
4) The using of the correlations from literature for the calculus of (V_{mf}), does not predict the (V_{mf}) adequately for the specific mixtures used in this study. The empirical model for predicting

the minimum fluidization velocity of sand and sugarcane bagasse mixture was developed considering the relationship between Reynolds number at minimum fluidization velocity (R_{emf}) and Archimedes number (A_r). The experimental error and the predicted values shows that the equation predict 88% of the experimental conditions tested, with errors lowers or close to 30% of the experimental value. The results were not satisfactory for the case of mixture with very small sugarcane particles (≥0.15 mm) in mixtures ranges 2–15% of mass fraction of bagasse.

Acknowledgements

The authors are grateful to the Coordination for the Improvement of Higher Education Personnel (CAPES), from the Brazilian Ministry of Education (MEC), and to the National Council for Scientific and Technological Development (CNPq) (process 150223/2017-0) from the Ministry of Science and Technology (MCT) because of their generous financial support to this research. In addition, the authors highly appreciate Mr. Fernando Araujo for his help and support to carry out the experimental analysis.

References

[1] H. Cui, J.R. Grace, Fluidization of biomass particles: a review of experimental multiphase flow aspects, Chem. Eng. Sci. 62 (1–2) (2007) 45–55.
[2] C.A.S. Felipe, S.C.S. Rocha, Prediction of minimum fluidization velocity of gas-solid fluidized beds by pressure fluctuation measurements - analysis of the standard deviation methodology, Powder Technol. 174 (3) (2007) 104–113.
[3] S. Heidenreich, P.U. Foscolo, New concepts in biomass gasification, Prog. Energy Combust. Sci. 46 (2015) 72–95.
[4] Y. Xue, S. Zhou, R.C. Brown, A. Kelkar, X. Bai, Fast pyrolysis of biomass and waste plastic in a fluidized bed reactor, Fuel 156 (2015) 40–46.
[5] J. Van Caneghem, A. Brems, P. Lievens, C. Block, P. Billen, I. Vermeulen, R. Dewil, J. Baeyens, C. Vandecasteele, Fluidized bed waste incinerators: design, operational and environmental issues, Prog. Energy Combust. Sci. 38 (4) (2012) 551–582.
[6] K. Zhang, B. Yu, J. Chang, G. Wu, T. Wang, D. Wen, Hydrodynamics of a fluidized bed co-combustor for tobacco waste and coal, Bioresour. Technol. 119 (2012) 339–348.
[7] W. Zhong, B. Jin, Y. Zhang, X. Wang, R. Xiao, Fluidization of biomass particles in a gas-solid fluidized bed, Energy & Fuels 22 (6) (2008) 4170–4176.
[8] B. Paudel, Z.-G. Feng, Prediction of minimum fluidization velocity for binary mixtures of biomass and inert particles, Powder Technol. 237 (2013) 134–140.
[9] K.L. Clarke, T. Pugsley, G.A. Hill, Fluidization of moist sawdust in binary particle systems in a gas–solid fluidized bed, Chem. Eng. Sci. 60 (24) (2005) 6909–6918.
[10] C.R. Cardoso, T.J.P. Oliveira, J.A. Santana Junior, C.H. Ataíde, Physical characterization of sweet sorghum bagasse, tobacco residue, soy hull and fiber sorghum bagasse particles: density, particle size and shape distributions, Powder Technol. 245 (2013) 105–114.
[11] A.M. Sharma, A. Kumar, K.N. Patil, R.L. Huhnke, Fluidization characteristics of a mixture of gasifier solid residues, switchgrass and inert material, Powder Technol. 235 (2013) 661–668.
[12] A.W. Nienow, P.N. Rowe, L.Y.L. Cheung, A quantitative Analysis of the mixing of two segregating powders of different density in a gas fluidised bed, Powder Technol. 20 (1978) 89–97.
[13] K.V.N.S. Rao, G.V. Reddy, Cold flow studies of rice husk, saw dust, and groundnut shell Fuels in a fluidized bed, Energy Sources, Part A Recover. Util. Environ. Eff. 32 (18) (2010) 1701–1711.
[14] M. Hartman, O. Trnka, M. Pohořelý, Minimum and terminal velocities in fluidization of particulate ceramsite at ambient and elevated temperature, Ind. Eng. Chem. Res. 46 (22) (2007) 7260–7266.
[15] Y. Zhang, W. Zhong, B. Jin, Experimental and theoretical study on fluidization of stalk-shaped biomass particle in a fluidized bed, Int. J. Chem. React. Eng. 9 (1) (2011).
[16] M. Hartman, M. Pohořelý, O. Trnka, Fluidization of dried wastewater sludge, Powder Technol. 178 (3) (2007) 166–172.
[17] T.R. Rao, J.V. Ram Bheemarasetti, Minimum fluidization velocities of mixtures of biomass and sands, Energy 26 (6) (2011) 633–644.
[18] J. Pilar Aznar, M. Gracia-Gorria, F.A. Corella, Minimum and maximum velocities for fluidization for mixtures of agricultural and forest residues with second fluidized solid. I. Preliminary data and results with sand-sawdust mixtures, Int. Chem. Eng. 32 (1992) 95–102.
[19] V.S. Chok, A. Gorin, H.B. Chua, Minimum and complete fluidization velocity for sand-palm shell mixtures, Part II: characteristic velocity profiles, Crit. Load. Bin. Correl. Am. J. Appl. Sci. 7 (6) (2010) 773–779.
[20] O.M. Todes, Applications of fluidized beds in the chemical industry, part II, Leningr. Izd. Zn. (1995) 4–27.
[21] B.J. Ramakers, R. de Ridder, P.J.A.M. Kerkhof, Fluidization behavior of wood/sand mixtures, in: Proceeding of the 14th International Drying Symposium, 2004, pp. 1337–1344.
[22] F.C. Woh, J. Janaun, A. Prabhakar, K. Krishnaiah, Minimum fluidization velocity of plam kernel cake particles in fluidized bed fermenter, J. Appl. Sci. 7 (2007) 2183–2187.
[23] C. Si, Q. Guo, Fluidization characteristics of binary mixtures of biomass and quartz sand in an acoustic fluidized bed, Ind. Eng. Chem. Res. 47 (23) (2008) 9773–9782.
[24] Centro de Tecnologia Canavieira, Censo Varietal de Productividade, 2011.
[25] O. Kunii, D. Levenspiel, Fluidization Engineering, second ed., 1991. Butterworth, Heinemann.
[26] D. Geldart, Gas Fluidization Technology, John Wiley and Sons, 1986.
[27] B.H.W. Bernhardt, Shape factors of bagasse particles, in: Proceedings of The South African Sugar Technologists', 1993.
[28] ASTM E873-82, Standard Test Method for Bulk Density of Densified Particulate Biomass Fuels, 2013. Reapproved.
[29] B. Rodieck, EllipseFitter class of ImageJ, Accessed Maio, http://rsb.info.nih.gov/ij/developer/source/ij/process/EllipseFitter.java.html, 2016.
[30] H. Heywood, Size, Shape and Size Distribution of Particulate Materials. Course on Particle Technology, 1970. Nordwijk, Netherlands.
[31] C. Igathinathane, L.O. Pordesimo, E.P. Columbus, W.D. Batchelor, S. Sokhansanj, Sieveless particle size distribution analysis of particulate materials through computer vision, Comput. Electron. Agric. 66 (2) (2009) 147–158.
[32] D. Geldart, Types of gas fluidization, Powder Technol. 7 (1973) 285–292.
[33] S. Ergum, Fluid flow through packed columns, Chem. Eng. Prog. 48 (1952) 89–94.
[35] G.L. Goossens, W.R.A. Dumont, G.L. Spaepen, Fluidization of binary mixtures in laminar flow region, Chem. Eng. Prog. Symp. 67 (1971) 38–45.
[37] S.P. Babu, B. Shah, A. Talwalker, Fluidization correlations for coal gasification materials — minimum fluidization velocity and fluidized bed expansion ratio, Chem. Eng. Prog. Symp. 74 (1978) 176–186.
[38] D.C. Chitester, R.M. Kornodky, Characteristics of fluidization at high pressure, Chem. Eng. Sci. 39 (2) (1984) 253–261.
[39] J.R. Grace, Handbook of Multiphase Systems, Hemisphere Pub. Corp., Washington DC, 1986.
[40] P.G.P. Bourgeoi, Ratio of terminal velocity to minimum fluidization velocity for spherical particles, Can. J. Chem. Eng. 46 (1968) 325–329.
[41] M.A.D.S. Jeronimo, J.F. Richardson, Velocity-voidage relations for sedimentation and fluidization, Chem. Eng. Sci. 34 (1979) 1419–1422.
[42] L.P.A. Lucas, J. Arnaldos, J. Casal, High temperature incipient fluidization in mono and poly disperse systems, Chem. Eng. Community 41 (1986) 121–132.
[43] J. Reina, E. Velo, L. Puigjaner, Predicting the minimum fluidization velocity of polydisperse mixtures of scrap-wood particles, Powder Technol. 111 (2000) 245–251.
[44] B. Formisani, R. Girimonte, T. Longo, The fluidization pattern of density-segregating binary mixtures, Chem. Eng. Res. Des. 86 (4) (2008) 344–348.
[45] B. Formisani, R. Girimonte, T. Longo, The fluidization process of binary mixtures of solids: Development of the approach based on the fluidization velocity interval, Powder Technol. 185 (2) (2008) 97–108.
[46] Y. Zhang, B. Jin, W. Zhong, Experimental investigation on mixing and segregation behavior of biomass particle in fluidized bed, Chem. Eng. Process. Process Intensif. 48 (3) (2009) 745–754.
[47] A. Rao, J.S. Curtis, Classifying the fluidization and segregation behavior of binary mixtures using particle size and density ratios, AIChE J. 57 (6) (2011) 1446–1458.
[48] P.N. Rowe, A.W. Nienow, Particle mixing and segregation in gas fluidised beds, A Rev. Powder Technol. 15 (2) (1976) 141–147.
[49] A.W. Nienow, P.N. Rowe, L.Y.L. Cheung, A quantitative analysis of the mixing of two segregating powders of different density in a gas-fluidised bed, Powder Technol. 20 (1) (1978) 89–97.
[50] L. Huilin, H. Yurong, D. Gidaspow, Y. Lidan, Q. Yukun, Size segregation of binary mixture of solids in bubbling fluidized beds, Powder Technol. 134 (1–2) (2003) 86–97.
[51] B. Formisani, G.D. Cristofaro, R. Girimonte, A fundamental approach to the phenomenology of fluidization of size segregating binary mixtures of solids, Chem. Eng. Sci. 56 (1) (2001) 109–119.
[52] G. Olivieri, A. Marzocchella, P. Salatino, Segregation of fluidized binary mixtures of granular solids, AIChE J. 50 (12) (2004) 3095–3106.
[53] V. Chok, S.K. Wee, A. Gorin, H.B. Chua, Effect of particle and bed diameter on characteristic velocities in compartmented fluidized bed gasifier, Pertanika J. Sci. Technol. 17 (2) (2009) 347–354.
[54] V.S. Chok, A. Gorin, H.B. Chua, Minimum and complete fluidization velocity for sand-palm shell mixtures, Part I: fluidization behavior and characteristic velocities, Am. J. Appl. Sci. 7 (6) (2010) 763–772.
[55] M.G. Rasul, V. Rudolph, M. Carsky, Segregation potential in binary gas fluidized beds, Powder Technol. 103 (2) (1999) 175–181.
[56] B. Formisani, R. Girimonte, V. Vivacqua, Fluidization of mixtures of two solids differing in density or size, AIChE J. 57 (9) (2011) 2325–2333.
[57] F.P. Di Maio, A. Di Renzo, V. Vivacqua, A particle segregation model for gas-fluidization of binary mixtures, Powder Technol. 226 (2012) 180–188.

[58] A. Di Renzo, F.P. Di Maio, R. Girimonte, V. Vivacqua, Segregation direction reversal of gas-fluidized biomass/inert mixtures – experiments based on Particle Segregation Model predictions, Chem. Eng. J. 262 (2015) 727–736.
[60] N.P. Pérez, E.B. Machin, D.T. Pedroso, J.S. Antunes, J.L. Silveira, Fluid-dynamic assessment of sugarcane bagasse to use as feedstock in bubbling fluidized bed gasifiers, Appl. Therm. Eng. 73 (1) (2014) 238–244.
[61] D.A. Nemtsov, A. Zabaniotou, Mathematical modelling and simulation approaches of agricultural residues air gasification in a bubbling fluidized bed reactor, Chem. Eng. J. 143 (1–3) (2008) 10–31.
[62] F. Fotovat, J. Chaouki, J. Bergthorson, The effect of biomass particles on the gas distribution and dilute phase characteristics of sand-biomass mixtures fluidized in the bubbling regime, Chem. Eng. Sci. 102 (2013) 129–138.
[63] S.M. Beheshti, H. Ghassemi, R. Shahsavan-Markadeh, Process simulation of biomass gasification in a bubbling fluidized bed reactor, Energy Convers. Manag. 94 (2015) 345–352.
[64] C. Loha, S. Gu, J. De Wilde, P. Mahanta, P.K. Chatterjee, Advances in mathematical modeling of fluidized bed gasification, Renew. Sustain. Energy Rev. 40 (2014) 688–715.
[65] A. Marzocchella, P. Salatino, V. Di Pastena, L. Lirer, Transient fluidization and segregation of binary mixtures of particles, AIChE J. 46 (11) (2000) 2175–2182.
[67] L. Jones, L.R. Glicksman, An experimental investigation of gas flow in a scale model of a fluidized-bed combustor, Powder Technol. 45 (3) (1986) 201–213.
[68] L.R. Glicksman, M.R. Hyre, K. Woloshun, Simplified scaling relationships for fluidized beds, Powder Technol. 77 (2) (1993) 177–199.
[69] L.R. Glicksman, M.R. Hyre, P.A. Farrell, Dynamic similarity in fluidization, Int. J. Multiph. Flow. 20 (1) (1994) 331–386.
[70] M. Jiliang, C. Xiaoping, L. Daoyin, Minimum fluidization velocity of particles with wide size distribution at high temperatures, Powder Technol. 235 (2013) 271–278.
[71] B. Formisani, R. Girimonte, L. Mancuso, Analysis of the fluidization process of particle beds at high temperature, Chem. Eng. Sci. 53 (5) (1998) 951–961.
[72] H.J. Subramani, M.B. Mothivel Balaiyya, L.R. Miranda, Minimum fluidization velocity at elevated temperatures for Geldart's group-B powders, Exp. Therm. Fluid Sci. 32 (1) (2007) 166–173.
[73] G. Bruni, R. Solimene, A. Marzocchella, P. Salatino, J.G. Yates, P. Lettieri, M. Fiorentino, Self-segregation of high-volatile fuel particles during devolatilization in a fluidized bed reactor, Powder Technol. 128 (1) (2002) 11–21.
[74] R. Girimonte, B. Formisani, Effects of operating temperature on the bubble phase properties in fluidized beds of FCC particles, Powder Technol. 262 (2014) 14–21.